

# Concerted supramolecular motifs: linear columns and zigzag chains of multiple phenyl embraces involving $\text{Ph}_4\text{P}^+$ cations in crystals†

Ian Dance\* and Marcia Scudder

School of Chemistry, University of New South Wales, Sydney 2052, Australia

One-dimensionally infinite sequences of mutually *attractive*  $\text{Ph}_4\text{P}^+$  cations occur in crystals, as independent supramolecular motifs. These motifs involve concerted, multiple phenyl embraces, based on the intermolecular edge-to-face (**ef**) interaction between phenyl groups. The linear infinite translational quadruple phenyl embrace (LITQPE) has four **ef** interactions between each pair of  $\text{Ph}_4\text{P}^+$  ions, propagated in almost all cases by lattice translation. In the zigzag infinite sextuple phenyl embrace (ZZISPE), each  $\text{Ph}_4\text{P}^+$  presents three phenyl groups to each of its neighbours, and there are six **ef** interactions between each pair of cations which are commonly related by a centre of inversion: the infinite sequence of P atoms is planar with approximately tetrahedral angles. In crystals, LITQPE columns and ZZISPE chains are usually parallel to stacks of anions, which vary in size from  $\text{Br}^-$  to  $[(\mu_6\text{-C})\text{Os}_{10}(\text{CO})_{24}\text{HgCF}_3]^-$ : the anion stack can contain solvent, or the anion can be one-dimensionally non-molecular. 52 Crystals containing isolated LITQPE columns and 36 crystals containing ZZISPE chains have been described, and crystal packing types (supramolecular crystal isomers) classified. The cation motifs are not disordered, whereas associated anions can be. Strong attractions exist between  $\text{Ph}_4\text{P}^+$  cations within these two motifs. Calculated through-space energies for typical structures are *ca.* 13 kcal mol<sup>-1</sup> net attraction per  $[\text{Ph}_4\text{P}^+]_2$  pair within a LITQPE, and *ca.* 16 kcal mol<sup>-1</sup> net attraction within a ZZISPE. In contrast, the strongest interactions between these isolated motifs are *ca.* 1–3 kcal mol<sup>-1</sup> attraction for the closest intermotif pair of  $\text{Ph}_4\text{P}^+$  cations. The intramotif attractive energies have similar magnitude to the cation–anion attractive energies. The LITQPE and ZZISPE can be regarded as supramolecular crystal tectons, energetically comparable with hydrogen bonds.

In two previous papers we have described the multiple phenyl embrace (MPE) involving pairs of  $\text{Ph}_4\text{P}^+$  cations in crystals.<sup>1,2</sup> These are strongly attractive concerted supramolecular motifs. The conformations of phenyl rings in  $\text{Ph}_4\text{P}^+$ , while partially restricted by intracation phenyl–phenyl interactions,<sup>3,4</sup> are able to support five types of MPE in which intercation pairs of phenyl rings engage in attractive edge-to-face (**ef**) and offset face-to-face (**off**) interactions. The dominant MPE is the sextuple phenyl embrace (SPE), illustrated in Fig. 1(a), in which three rings of each cation have **ef** interactions with three rings of the other (often across a centre of inversion). Each phenyl ring in the SPE domain is involved in one edge  $\Rightarrow$  face interaction and one face  $\Leftarrow$  edge interaction, as illustrated by the arrows in Fig. 1(a). Sextuple phenyl embraces typically have net attractive energies in the range 15 to 20 kcal mol<sup>-1</sup> per  $[\text{Ph}_4\text{P}^+]_2$  pair, and P...P separations in the range 5.8 to 6.8 Å.<sup>1</sup> The prevalence of this motif is demonstrated by the statistics of occurrence: in the Cambridge Structural Database (CSD),<sup>5</sup> of 770 compounds containing  $\text{Ph}_4\text{P}^+$  (and with coordinates available, in 1994), 489 structures contain 812 different instances of P...P separations less than 7 Å, and 86% of these are SPE.<sup>2</sup> Another key MPE for  $\text{Ph}_4\text{P}^+$  is the translational quadruple embrace (TQPE)<sup>2</sup> involving four rings (two from each cation) and four **ef** interactions in the embrace region [see Fig. 1(b)]: the crystallographic relationship between the two cations involved in this embrace is frequently translation, and cannot be a centre of inversion. The TQPE uses the pseudo-two-fold axis of  $\text{Ph}_4\text{P}^+$  rather than the pseudo-three-fold axis of the SPE, and consequently

is slightly longer with a P...P separation of 6.7–7.9 Å: the attractive energy of a TQPE is 10–16 kcal mol<sup>-1</sup> per  $[\text{Ph}_4\text{P}^+]_2$  pair.

A  $\text{Ph}_4\text{P}^+$  cation is able to participate in more than one multiple phenyl embrace, often two or three, and the structures of crystals containing  $\text{Ph}_4\text{P}^+$  frequently contain chains and networks of such embraces. These are previously unrecognised supramolecular motifs, which have strong influences on crystal packing. In this paper we describe one-dimensionally infinite chains of multiple phenyl embraces, specifically the zigzag infinite sextuple phenyl embrace (ZZISPE) and the linear infinite translational quadruple phenyl embrace (LITQPE), and their occurrence as distinct supramolecular features of crystal structures in the Cambridge Structural Database. In a subsequent paper we will describe the more elaborate networks of multiple phenyl embraces in crystals.<sup>6</sup> The objective in this paper is to define and characterise these new motifs, and to identify the patterns of their occurrence in crystals. This research seeks a predictive understanding of the structures of crystals containing  $\text{Ph}_4\text{P}^+$ , and the ability to design and engineer crystal structures.<sup>7–9</sup>

## Methodology

Information was drawn from the August 95 graphical version of the CSD,<sup>5</sup> in which there are more than 849 crystals containing  $\text{Ph}_4\text{P}^+$  (and with atomic coordinates available). Details of the interrogation of the CSD in order to identify the SPE and TQPE and extract structures containing them have been provided previously.<sup>1,2</sup> The criteria for inclusion of SPEs here are that P...P  $\leq 7$  Å, and the mean of the two P...P–C<sub>distal</sub> angles be in the range 160–180°. For TQPE the criteria are that there be four interacting rings in an **ef** arrangement, and that P...P  $\leq 8$  Å. The criterion for selection of separated chains was that interchain P...P distances be  $>9$  Å. The crystal lattices were generated,

† Supplementary data available (No. SUP 57160, 7 pp.): alphabetical list of REFCODES and refs. for the tabulated compounds and Table of miscellaneous instances of separated LITQPE columns in crystals. See Instructions for Authors, *J. Chem. Soc., Dalton Trans.*, 1996, Issue 1. Non-SI unit employed: kcal = 4.18 kJ.

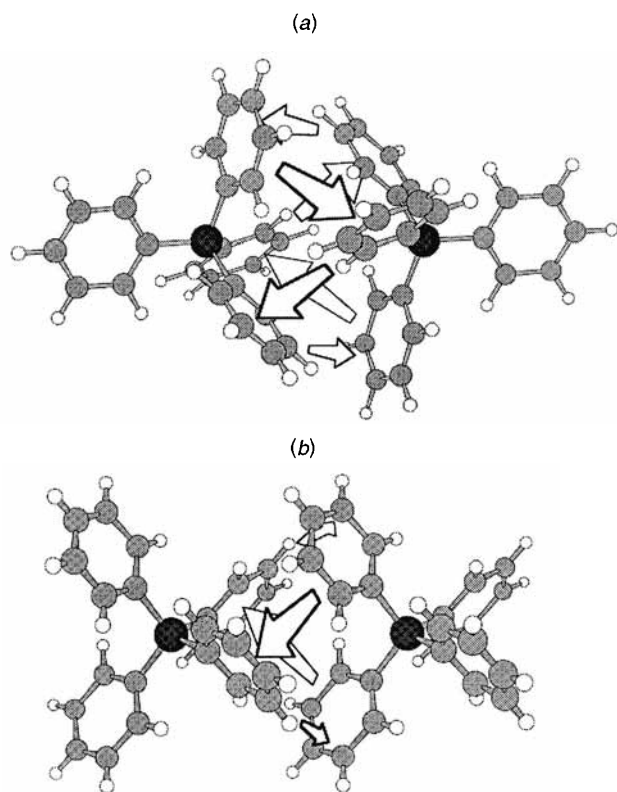


**Fig. 1** (a) Representative SPE between two  $\text{Ph}_4\text{P}^+$  cations, recognisable by the virtual collinearity of the two P–C bonds of the distal phenyl groups not involved in the SPE. The  $\text{P}\cdots\text{P}$  separation is 6.4 Å, across a centre of inversion. The arrows mark the six phenyl–phenyl interactions between the cations, which provide the main attractive energy. (b) Representative TQPE involving four phenyl rings in *ef* interactions (arrowed)

examined and displayed using modules of the ‘Catalysis’ software from MSI.<sup>10</sup>

Compounds are most simply identified by their reference codes (REFCODES) from the CSD; chemical formulas are provided in the tables. Literature references, identified by the REFCODES, are listed in SUP 57160.

The calculations of intermolecular energies<sup>11</sup> used standard atom–atom methodology<sup>7,9,12,13</sup> with the Lennard–Jones equation  $E_{ij}^{\text{dW}} = e^a_{ij}[(d^a_{ij}/d_{ij})^{12} - 2(d^a_{ij}/d_{ij})^6]$  for the van der Waals components and the equation  $E_{ij} = \{q_i q_j\}/(\epsilon d_{ij})$  for the coulombic components, for atoms  $i, j$  with partial charges  $q_i, q_j$ , separated by  $d_{ij}$ ;<sup>9</sup>  $d^a_{ij}$  is the distance at which the interaction energy is most negative (attractive) with the magnitude  $e^a_{ij}$ ;  $d^a_{ij} = r^a_i + r^a_j$ ;  $e^a_{ij} = (e^a_i e^a_j)^{0.5}$ ; the intermolecular relative permittivity  $\epsilon$  was set as  $d_{ij}$ . The relevant van der Waals parameters  $r^a$  (Å) and  $e^a$  (kcal mol<sup>-1</sup>) respectively were: H 1.50, 0.040; C 2.00, 0.050; P 2.10, 0.20; Nb 2.10, 0.20; S 2.10, 0.20; Cl bonded 2.10, 0.20; As 2.10, 0.20; covalently bonded Br 2.30, 0.21; Br in  $\text{Br}^-$  2.50, 0.25. Justificatory discussion of these parameters for the cations has been presented.<sup>2,9</sup> The van der Waals parameters for the metal and Group 15, 16 and 17 atoms in the anions were selected to be consistent, according to periodic variation, with best values from established force-field development.<sup>13–15</sup> The partial charges used for the coulombic energies were:  $\text{H}^{+0.15}$ ,  $\text{C}^{-0.1}$ ,  $\text{P}^{+0.4}$  in  $\text{Ph}_4\text{P}^+$ ;  $\text{Br}^{-1.0}$  in  $\text{Br}^-$ ;  $\text{Nb}^{+1.5}$ ,  $\text{S}^{-0.5}$ ,  $\text{Cl}^{-0.5}$  in  $[\text{NbCl}_6]^-$ ;  $\text{Nb}^{+1.4}$ ,  $\text{Cl}^{-0.4}$  in  $[\text{NbCl}_6]^-$ ;  $\text{Nb}^{+0.8}$ ,  $\text{Cl}^{-0.3}$  in  $[\text{NbBr}_6]^-$ ;  $\text{As}^{+0.83}$ ,  $\text{S}^{-0.5}$ ,  $\text{Cl}^{-0.5}$  in  $[\text{As}_3\text{S}_3\text{Cl}_4]^-$ . Assignment of these charges was performed by density functional calcu-

\* Double numerical basis sets with polarisation functions, and the Becke, Lee–Yang–Parr functionals.<sup>16</sup>

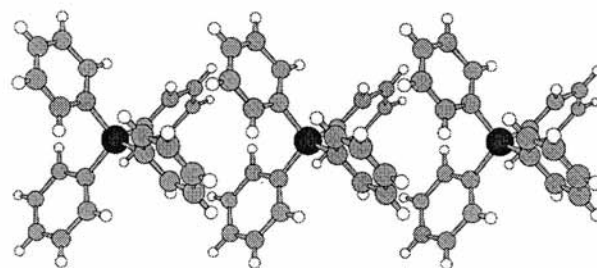


**Fig. 2** Part of a LITQPE showing three  $\text{Ph}_4\text{P}^+$  cations: the repeat unit is one cation, or one TQPE comprising four phenyl rings involved in four *ef* intermolecular interactions

lations\* with Mulliken analysis, and by concepts of chemical periodicity.†

## Results

Examination of the CSD shows that there are two common one-dimensional sequences of MPE, namely the LITQPE and the ZZISPE. These are almost invariably infinite. Our presentation of these focuses on two characteristics, namely the properties (geometry, symmetry, energy) of the individual chains, and the packing of the chains and the anions (and sometimes solvent) in the crystal lattices.

Fig. 2 shows a typical sequence of three  $\text{Ph}_4\text{P}^+$  involved in LITQPE interactions. The translational repetition is obvious, and it is common for the repeat unit of the LITQPE to be the lattice repeat. However there is a small number of LITQPE interactions in which a crystallographic  $2_1$  screw axis is the propagating operation. Translation requires that the  $\text{P}\cdots\text{P}\cdots\text{P}$  angles be 180°, while the  $2_1$  propagation allows small deviations from linearity: because the LITQPE is actually or almost linear this motif is described as a column.

Fig. 3 shows end and side views of a representative ZZISPE. The  $\text{Ph}_4\text{P}^+$  are arranged in a zigzag such that each  $\text{Ph}_4\text{P}^+$  presents three phenyl groups to each of its neighbours, and is able to form two very good SPEs. At each  $\text{Ph}_4\text{P}^+$  along a ZZISPE, two phenyl rings are common to two SPEs and are close to the central axis of the zigzag, while the other two phenyl groups are on the surface of the chain: the outer phenyl rings at each P along the ZZISPE are the distal phenyl groups of the individual SPEs. The zigzag geometry of the ZZISPE is a consequence of the tetrahedral disposition of phenyl groups at P, and the  $\text{P}\cdots\text{P}\cdots\text{P}$  angles could be expected to approach the tetrahedral angle. A significant characteristic of the ZZISPE is that the P atoms are coplanar: helical sequences are not permitted by the requirements of the SPE. As will be seen, various crystallographic symmetry operations can propagate the ZZISPE, but the most common is a centre of inversion. The ZZISPE has a characteristic view when projected along the axis, apparent in Fig. 3 and later figures.

### Characteristics of LITQPE columns

We have identified 54 good instances of isolated LITQPE columns, with  $\text{P}\cdots\text{P}$  separations within the QPEs ranging from 6.7 to 7.9 Å.‡ These LITQPE are classified according to the crystal lattices in which they occur, which are correlated also to some extent with the characteristics of the associated anions. The three main classes are those in space group  $P4/n$ , collected in Table 1, those in space group  $I4$  in Table 2, those in space

† The calculated energies are relatively insensitive to charge assignments: for instance in  $\text{Ph}_4\text{P}^+[\text{NbCl}_6]^-$ , the through-space energy between an anion and the nearest cation is –13.0 kcal mol<sup>-1</sup> for charges  $\text{Nb}^{+0.8}$ ,  $\text{Cl}^{-0.3}$  and –13.3 kcal mol<sup>-1</sup> for charges  $\text{Nb}^{+2.6}$ ,  $\text{Cl}^{0.6}$ .

‡ We have not investigated weaker LITQPEs longer than 8 Å.

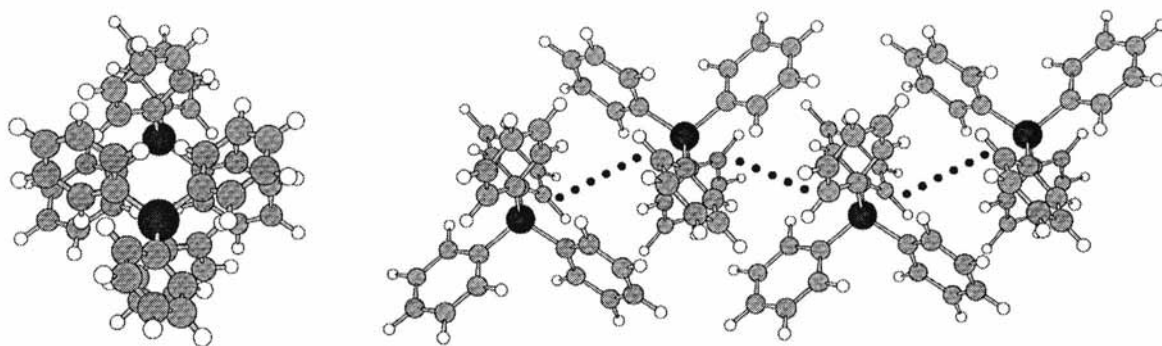


**Fig. 3** End and side views of part of a ZZISPE of  $\text{Ph}_4\text{P}^+$  cations. The SPE interactions marked as  $\text{P} \cdots \text{P}$  on the front view each involve three phenyl rings from each cation, and all of the P atoms are coplanar. The distal phenyl groups which are approximately collinear with each SPE are on the outside of the ZZISPE

**Table 1** Instances of LITQPE in space group  $P4/n$ . These structures are ordered in terms of increasing  $\text{P} \cdots \text{P}$  separation. All distances are in Å

REFCODE	Anion	$\text{P} \cdots \text{P}$ separation <sup>a</sup>	Cell length $a$	Comments <sup>b</sup>
COTDAQ	$[\text{ONbCl}_4(\text{OH}_2)]^-$	7.34	13.1	$\text{OH}_2$ of anion cannot obey $C_4$ symmetry of anion; H atoms not included in the CSD {GAYZUB packing}
BOSKOJ	$[\text{HCr}(\text{CO})_5]^-$	7.47	13.2	{CETBAE packing}
TACZOM	$[\text{AsCl}_6]^-$	7.52	13.1	{GAYZUB packing}
CETBAE	$[\text{SNbCl}_4]^-$	7.60	13.0	{CETBAE packing}
COYWAO	$[\text{OWCl}_4]^-$	7.60	12.7	{CETBAE packing}
PPHNOC	$[\text{OUCl}_3]^-$	7.62	13.3	{CETBAE packing}
FUYXAY	$[\text{SWCl}_4]^-$	7.63	12.9	{CETBAE packing}
CARFUW	$[\text{NMoCl}_4]^-$	7.65	12.8	{CETBAE packing}
POHWOY	$[\text{ReCl}_6]^-$	7.70	13.0	{GAYZUB packing}
CEXREC	$[\text{OsCl}_6]^-$	7.71	13.0	{GAYZUB packing}
ZZZAQD01	$[\text{OReCl}_4]^-$	7.71	12.7	{CETBAE packing}
JOPGAW	$[\text{B}_5\text{S}_4\text{H}_{10}]^-$	7.73	13.5	Anion disordered to maintain $C_4$ site symmetry {GAYZUB packing}
JATFIT	$[\text{WCl}_6]^-$	7.76	13.0	{GAYZUB packing}
BRNIMO	$[\text{NMoBr}_4]^-$	7.79	12.9	{CETBAE packing}
BUNHIB	$[\text{OMoBr}_4]^-$	7.84	12.9	{CETBAE packing}
BEVXIJ	$[\text{OVBr}_4]^-$	7.85	12.8	{CETBAE packing}
PCLNBA	$[\text{NbCl}_6]^-$	7.85	13.0	{GAYZUB packing}
GAYZUB	$[\text{S}_4\text{CB}_5\text{H}_{12}]^-$ (hetero-adamantane)	7.90	13.5	Anion disordered to maintain $C_4$ site symmetry {GAYZUB packing}

<sup>a</sup> The  $\text{P} \cdots \text{P}$  separation is the unit-cell length  $c$ . <sup>b</sup> See text for description of the GAYZUB and CETBAE packing sub-classification.

group  $C2/c$  in Table 3, while other miscellaneous instances of the LITQPE are tabulated in SUP 57160.

#### Separated LITQPE columns in tetragonal space group $P4/n$ .

In all of these crystals the LITQPEs occur as columns parallel to the tetragonal axis  $c$ , and the unique  $\text{P} \cdots \text{P}$  separation in each case is the  $c$ -axis length. Each cation has  $\bar{4}$  crystallographic site symmetry (point group  $S_4$ ). The anions are stacked along four-fold axes, and four parallel equivalent columns of LITQPE surround each stack of anions. Each anion has site symmetry 4 (point group  $C_4$ ). Fig. 4 shows the lattices projected along the tetragonal axis for two structures with anions  $[\text{SNbCl}_4]^-$  (CETBAE) and the hetero-adamantane cluster  $[\text{S}_4\text{CB}_5\text{H}_{12}]^-$  (GAYZUB). Table 1 gives the  $\text{P} \cdots \text{P}$  separations, the length of the cell  $a$  axis, and the identity of the anion for each of the structures in this class.

The  $a$ -axis lengths span the narrow range 12.7 to 13.5 Å, while the  $\text{P} \cdots \text{P}$  separations range from 7.34 to 7.90 Å: the lattices are formally isomorphous. Most of the anions are very similar, and in all except three cases the anion has point group symmetry  $C_4$ : in the exceptions (COTDAQ, JOGPAW and GAYZUB) the anion is disordered to comply with the site symmetry 4. Note that only anions, not cations, are disordered. In this structure type the tetragonal length of the monoanion cannot be greater than the  $\text{P} \cdots \text{P}$  separation in a TQPE, that is not greater than ca. 8 Å.

In this lattice type there is registry along  $c$  between all LITQPE columns of cations, but no translational registry is

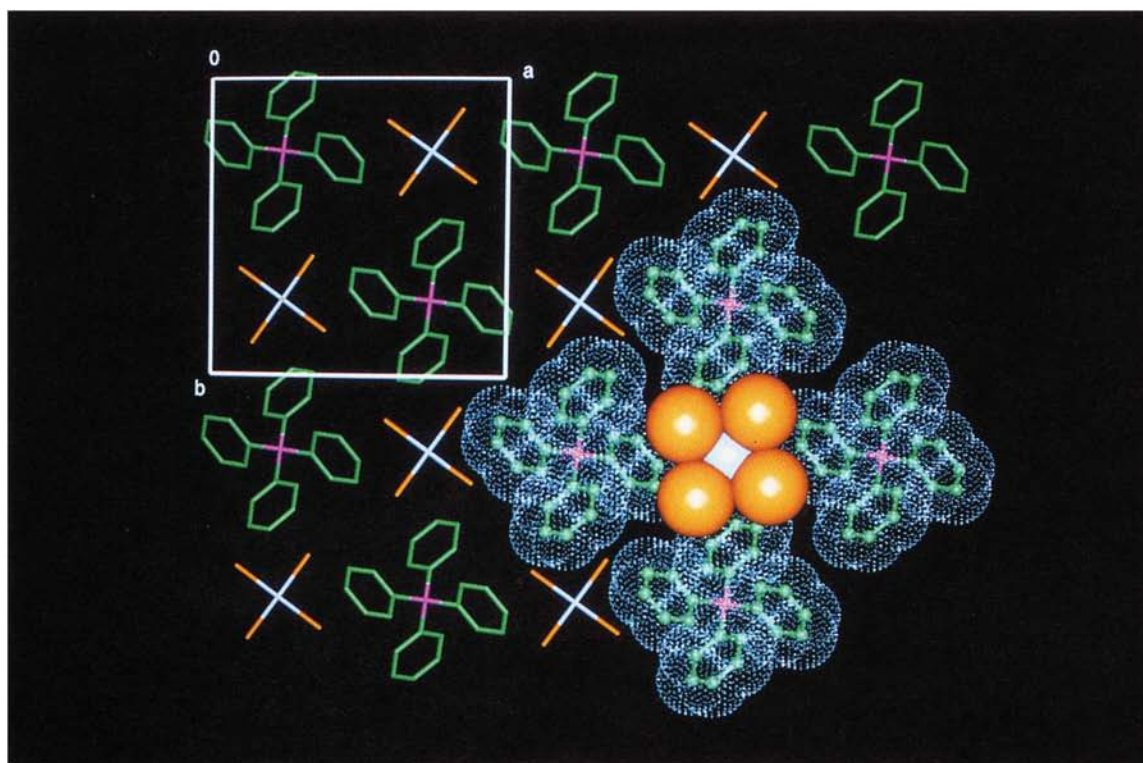
required between the cation columns and the anion stacks. The separation of the cation columns is  $a/\sqrt{2}$  (see Table 1), and the smallest such separation is 9.0 Å. The columns of LITQPE have rotational freedom around their axes, and there is variation as shown in Fig. 4 for CETBAE and GAYZUB. The phenyl-phenyl contacts between the columns are different for these two structures, and in fact the  $P4/n$  class of structures divides into two sub-classes, the CETBAE and GAYZUB classes shown in Fig. 4, with a packing difference described in terms of the rotations of the LITQPE columns. These sub-classes are identified in Table 1, where it can be seen that the compounds with an octahedral or effectively spherical anion belong to the GAYZUB class, while the compounds containing an anion which is chemically tetragonal ( $\text{AMB}_4$  or  $\text{AMB}_5$ ) belong to the CETBAE class.

#### Separated LITQPE columns in tetragonal space group $\bar{4}$ .

In this class there are columns of  $\text{Ph}_4\text{P}^+$  and stacks of anions parallel to the tetragonal axis, as in the  $P4/n$  class, but the symmetry and the details of the interactions are different. The cations and the anions are located at  $\bar{4}$  ( $S_4$ ) sites. Fig. 5 shows the simplest and tightest of these structures, with  $\text{Br}^-$  (DEMYEZ),\* and Table 2 provides details of members of this class.

\* A dimorph of  $\text{Ph}_4\text{P}^+\text{Br}^-$ , (DEMYEZ01)<sup>17</sup> contains connected ZZISPE chains, while  $\text{Ph}_4\text{P}^+\text{Br}^-(\text{H}_2\text{O})_2$  (VAXFAB) contains isolated ZZISPE chains.

(a)



(b)

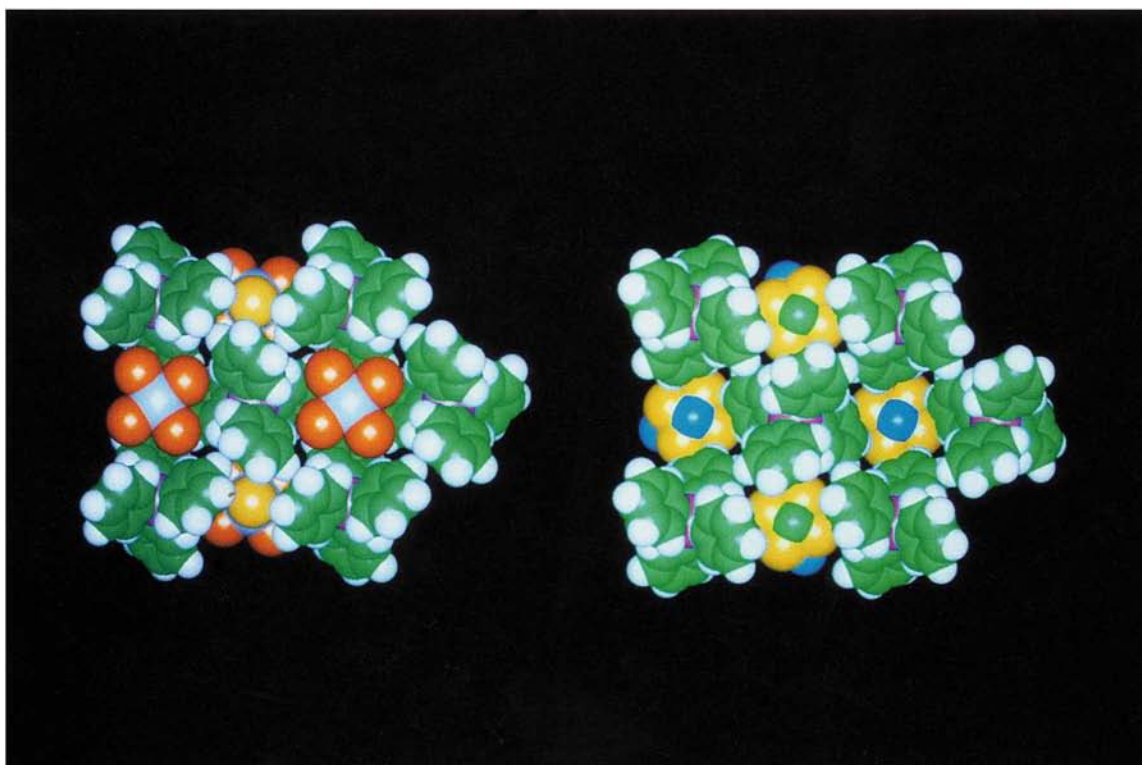


**Fig. 4** (a) Lattice packing for the LITQPE columns of  $\text{Ph}_4\text{P}^+$  cations and the stacks of anions in space group  $P4/n$ , viewed along the tetragonal axis. (b) Comparison of details of the different relationships between the packing of LITQPE columns and anion stacks in  $[\text{Ph}_4\text{P}]^+[\text{SNbCl}_4]^-$  (CETBAE, left; Nb grey, Cl orange, S yellow) and  $[\text{Ph}_4\text{P}]^+[\text{S}_4\text{CB}_5\text{H}_{12}]^-$  (GAYZUB, right; S yellow, B blue, C green, H omitted). One of the two disordered orientations of the  $[\text{S}_4\text{CB}_5\text{H}_{12}]^-$  anion along the four-fold axis is drawn. Notice that the four-fold array of LITQPE columns provides a cradle for the anion in each case, and that the two structures differ in details of the contacts *between* LITQPE columns, due to differing rotations of the columns about their axes

In this lattice type the four cations closest to the anion occur as a compressed tetrahedron, with  $\bar{4}$  symmetry. The four columns of LITQPE around a stack of monoanions effectively alternate in opposite directions, although the LITQPE is not strictly directional. It is this relationship between adjacent LITQPE, and the concomitant registry between the LITQPE

and the anion sites, which differentiates this group from the  $P4/n$  class. The separation of cation columns and of anion stacks is  $a/\sqrt{2}$ , slightly smaller than in the  $P4/n$  class.

It is apparent from Tables 1 and 2 that the  $\text{P}\cdots\text{P}$  distances along the LITQPE column in class  $\bar{4}$  are all shorter than those in class  $P4/n$ , and that the anions in class  $\bar{4}$  are generally

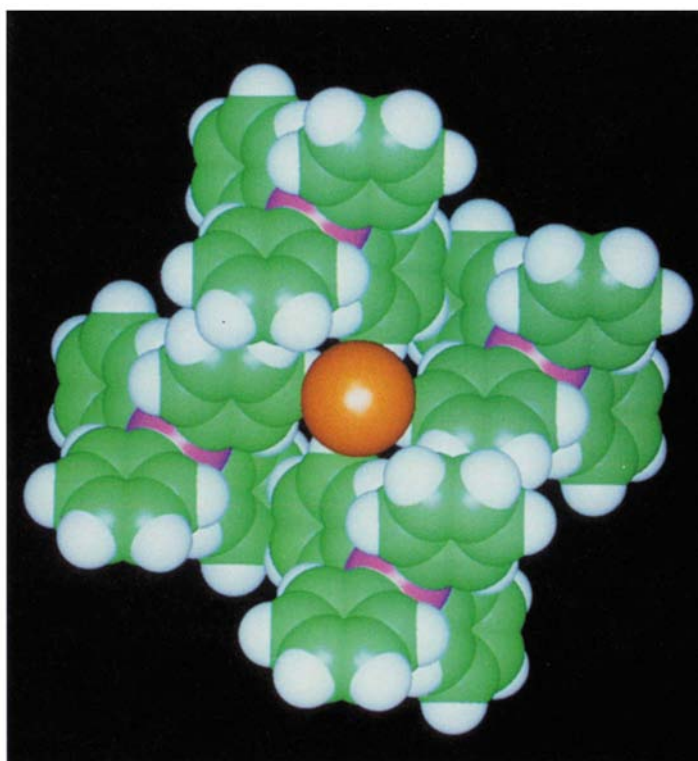


**Fig. 5** Projection along the tetragonal axis of the packing of LITQPE columns of  $\text{Ph}_4\text{P}^+$  and stacks of  $\text{Br}^-$  anions in crystalline  $\text{Ph}_4\text{P}^+\text{Br}^-$  (DEMYEZ), in space group  $I\bar{4}$ . Note that the array of four cations around each anion is different from that in Fig. 4

**Table 2** Tabulation for LITQPE, class  $I\bar{4}$ . These structures are ordered in terms of increasing  $\text{P}\cdots\text{P}^*$  separation. All distances are in Å

REFCODE	Anion	$\text{P}\cdots\text{P}^*$	Cell length $a$	Comments
KAZXOY	$\text{TeH}^-$	6.87	11.9	H atom not located, but the $\text{TeH}^-$ need not be disordered because the anion could lie along the $\bar{4}$ axis
SIGREF	$[\text{Hg}(\text{S}_2\text{WS}_2)_2]^{2-}$	6.95	13.2	Long anion with 2-, disordered: see text and Fig. 6
TPPHWS	$[\text{Zn}(\text{S}_2\text{WS}_2)_2]^{2-}$	6.89	13.3	As for isostructural SIGREF
WACTUP	$[\text{Mn}(\text{S}_2\text{WS}_2)_2]^{2-}$	6.96	13.2	As for isostructural SIGREF
DEMYEZ	$\text{Br}^-$	6.97	12.0	
SATSUB	$\text{I}^-$	6.98	12.0	
QQQEXJ01	$[\text{VO}_2\text{F}_2]^-$	7.14	12.2	Disorder of O, F
VUYJUJ	$[\text{PF}_6]^-$	7.17	12.2	
CIWZOX	$[\text{PS}_2\text{Br}_2]^-$	7.21	13.0	Disorder of S, Br
GEZMON	$[\text{FeCl}_4]^{2-}$ also $\text{H}^+$	7.22	13.0	Low quality structure determination: $\text{H}^+$ probably located in anion stack
WIBMUP	$[\text{Cr}^{\text{VO}}_3(\text{OH}_2)]^-$	7.31	12.3	Anion has four-fold disorder
WIBNAW	$[\text{Cr}^{\text{VO}}_3(\text{OH})]^-$	7.34	12.3	Anion has four-fold disorder

\* The unique  $\text{P}\cdots\text{P}$  separation along the column (= unit-cell length  $c$ ).

smaller than those in class  $P4/n$ , and have  $\bar{4}$  or pseudo- $\bar{4}$  symmetry. The crystal packing is tighter in class  $I\bar{4}$  than in class  $P4/n$ . There are weak *ef* phenyl–phenyl interactions between adjacent columns in DEMYEZ: these are apparent in Fig. 5, and their energies are evaluated below.

A neat illustration of the tightness of the LITQPEs and their packing is found in the three isomorphous compounds with larger dianions  $[\text{M}(\text{S}_2\text{WS}_2)_2]^{2-}$  ( $\text{M} = \text{Zn}, \text{Mn}$  or  $\text{Hg}$ ) (TPPHWS, SIGREF, WACTUP) illustrated in Fig. 6. Each anion is comprised of a row of three metal atoms,  $\text{W}-\text{M}-\text{W}$  along the stack, with tetrahedral  $\text{S}_4$  co-ordination of each metal, and overall symmetry  $\bar{4}$ . The anions are disordered in two ways in the anion stack. First, at each  $\text{W}$  atom location the two tetrahedra rotated by  $90^\circ$  about the stack axis are 50% populated. Secondly, the separation of  $[\text{M}(\text{S}_2\text{WS}_2)_2]^{2-}$  anions along the stack is such that  $\text{M}$  can occur equally between any adjacent pair of  $\text{WS}_4$  tetrahedra. This is equivalent to translational disorder of the anions by half an anion length along the stack, and can occur because the repeat length of the anions is commensurate with the cation repeat along the

LITQPE. The intriguing feature of this is that the narrow waist of the  $[\text{M}(\text{S}_2\text{WS}_2)_2]^{2-}$  anions, namely  $\text{M}$  at a  $\bar{4}$  site, threads closely through the narrowest region between cation columns: see Fig. 6. In fact the  $\text{Hg}$  atom is surrounded by eight  $\text{H}$  atoms of the phenyl rings of four different cations at distances of  $3.50 (\times 4)$  and  $3.67 (\times 4)$  Å. This has implications for the mechanism of crystallisation of these compounds. Note (Table 2) that the anions  $[\text{VO}_2\text{F}_2]^-$  and  $[\text{PS}_2\text{Br}_2]^-$  in this packing type are also disordered.

**Separated LITQPE columns in packing framework  $C2/c$ .** Parallel columns of LITQPE and stacks of anions also occur in monoclinic lattices in space group  $C2/c$ , in the compounds listed in Table 3. The cation columns are on two-fold axes parallel to the unique  $b$  axis, and therefore are linear with a  $\text{P}\cdots\text{P}$  distance equal to  $b$ . The anions are located on centres of symmetry, which in the case of the anions  $[\text{H}_3\text{GeM}(\text{CO})_5]^-$  ( $\text{M} = \text{Mo}$  or  $\text{W}$ ) requires disorder of the  $\text{H}_3\text{Ge}$  and *trans*- $\text{CO}$  ligands. The LITQPE in space group  $C2/c$  are separated by  $a/2$  (11.1–12.3 Å) and  $c/2$  (8.9–12.5 Å).

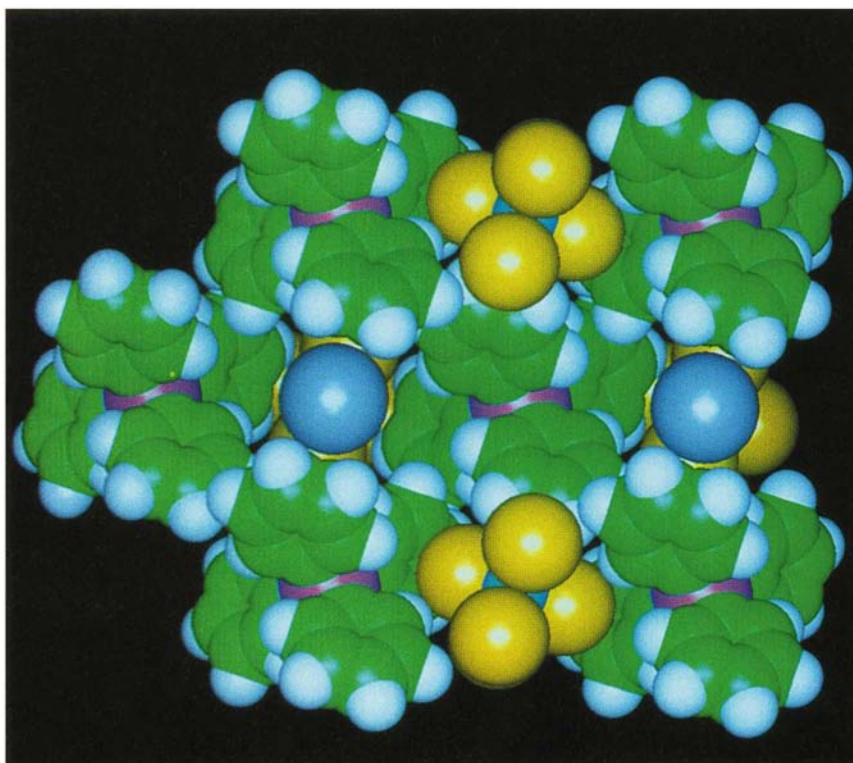


**Fig. 6** Representation of the crystal structure of  $[\text{Ph}_4\text{P}]_2[\text{Hg}(\text{S}_2\text{WS}_2)_2]$  (SIGREF), viewed along the tetragonal axis: Hg grey, S yellow, W obscured. In the upper and lower anions only one of the disordered conformations is drawn, while in the left and right molecules the upper  $\text{S}_2\text{WS}_2$  chelate is omitted to show how the Hg atom at the waist of the anion fits neatly between the LITQPE columns

**Table 3** Compounds containing separated LITQPE columns in the monoclinic lattice type  $C2/c$ . All distances are in Å and angles in °

REFCODE	Anion	P...P	Cell dimensions	Comments
PSBRNB	$[\text{NbBr}_6]^-$	6.86	23.0, 6.86, 17.8; 96.6*	Eight cations surround an anion centrosymmetrically, at Nb-P distances 6.88, 8.17, 8.65, 9.30
GAGVOZ	$[\text{UBr}_6]^-$	6.95	23.2, 7.0, 18.1; 96.4	In order to maintain centrosymmetry there is disorder of $\text{H}_3\text{Ge}$ and the <i>trans</i> CO
VAJWAE	$[\text{H}_3\text{GeMo}(\text{CO})_5]^-$	7.02	22.3, 7.0, 18.5; 96.1	
VAJWEI	$[\text{H}_3\text{GeW}(\text{CO})_5]^-$	7.03	22.2, 7.0, 18.5; 96.1	Isomorphous with VAJWEI
VUDTUJ	$[\text{AsBr}_4(\text{thf})_2]^-$	7.48	24.6, 7.5, 17.8; 94.0	The thf molecules extend from the anion stack between the cation columns
GANSET	$\infty\{\text{[Sb}_3\text{I}_{10}]^-\}$	7.45	23.7, 7.5, 25.0, 100.8	The repeat in the infinite anion matches the LITQPE separation: see text
FOJKOE	$[\text{Sb}_2\text{I}_8]^{2-} \cdot 2(\text{MeCN})$	6.86, 7.23 in linear column; 7.04 in non-linear column	45.6, 14.1, 19.9; 106.0	There are two distinct chains, linear along a 2 axis with doubled repeat, and non-linear along a $2_1$ axis, with P...P...P angles 178. Solvent molecules occur between anions

thf = Tetrahydrofuran. \* Transformed from the  $B2/b$  lattice reported.

In this class of LITQPE there is a lattice with included solvent (FOJKOE) and also a one-dimensionally non-molecular anion (GANSET). The crystal structure FOJKOE with  $[\text{Sb}_2\text{I}_8]^{2-} \cdot 2(\text{MeCN})$  (see Table 3) contains two distinct LITQPE columns, including a slightly non-linear infinite column of QPE propagated by a crystallographic  $2_1$  axis. In crystalline  $\text{Ph}_4\text{P}^+ \infty\{\text{[Sb}_3\text{I}_{10}]^-\}$  (GANSET) the repeat distance in the infinite anion matches the repeat distance of 7.45 Å in the LITQPE, allowing a commensurate lattice. However there is another distinctive property of this lattice which is informative: the LITQPE columns are forced apart by the increased cross-sectional area of the anion, as shown in Fig. 7: the separations of the LITQPE columns are now 11.9 and 12.5 Å, in contrast to the *ca.* 9 Å separation in the  $\bar{1}4$  and  $P4/n$  classes. The retention of the LITQPE shows them to be stable independent motifs.

Comparison of the crystal structures of  $\text{Ph}_4\text{P}^+[\text{NbCl}_6]^-$  ( $P4/n$ , Table 1) and  $\text{Ph}_4\text{P}^+[\text{NbBr}_6]^-$  ( $C2/c$ , Table 3) is informative. In the  $[\text{NbCl}_6]^-$  crystal in class  $P4/n$  the

octahedral anion is oriented with a four-fold axis parallel to the anion stack and the LITQPE direction: the  $\text{Cl} \cdots \text{Cl}$  through-space contact along the anion stack is at the van der Waals repulsive limit (3.25 Å) and the P...P separation (7.85 Å) is in the upper range. If the  $[\text{NbBr}_6]^-$  crystal adopted the same packing there would be conflict between anions compressed to repulsion along the stack (for a P...P separation of 7.85 Å the through-space  $\text{Br} \cdots \text{Br}$  contact would be an impossible 2.9 Å), or the TQPEs would be too elongated. Instead the  $[\text{NbBr}_6]^-$  crystal adopts the  $C2/c$  structure, in which the octahedral anion need not have a four-fold axis along the stacking direction, and can reorient with its three-fold axis parallel to the stacking direction. The shortest through-space  $\text{Br} \cdots \text{Br}$  contact is then 4.25 Å, and the P...P separation in the LITQPE can be reduced to a much more attractive 6.86 Å. On the other hand, if the  $[\text{NbCl}_6]^-$  compound adopted the  $C2/c$  structure the interanion  $\text{Cl} \cdots \text{Cl}$  distance along the anion stack would be *ca.* 4.5 Å, but this long value could not be reduced without unacceptable compression of the LITQPE.

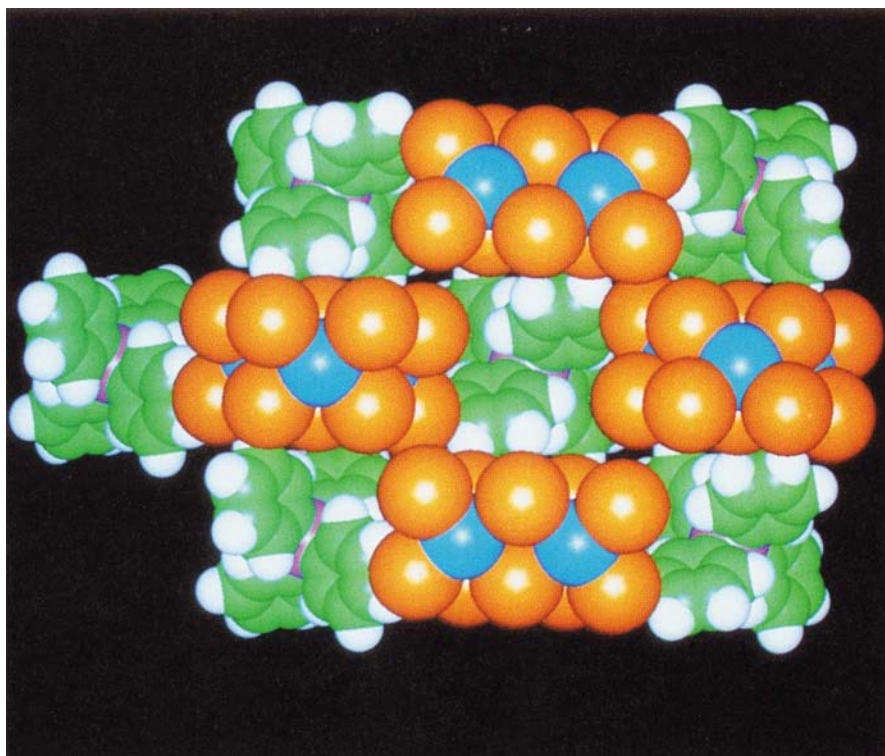
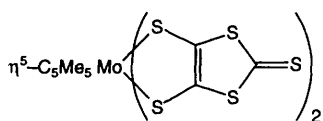


Fig. 7 Crystal packing of  $\text{Ph}_4\text{P}^+ \infty \{[\text{Sb}_3\text{I}_{10}]^-\}$  (GANSET), viewed along the LITQPE columns, which are separated by 11.9 and 12.5 Å

**Miscellaneous other LITQPE.** Seventeen other instances of separated LITQPE columns have been identified, for the following anions (+ solvent) (space group in parentheses) (see SUP 57160):  $[(\mu\text{-H})\text{W}_2(\text{CO})_{10}]^-$  ( $P\bar{4}$ );  $[\text{S}_3\text{N}_3]^-$  ( $P\bar{4}$ );  $[(\eta^5\text{-C}_5\text{Me}_5)\text{Mo}(\text{C}_3\text{S}_5)_2]^-$  ( $P\bar{4}$ );  $\mu$ -iodo-bis(*N*-iodosuccinim-



ide) + MeCN ( $Pna2_1$ );  $[\text{OMoCl}_4(\text{dmf})]^-$  (dmf = *N,N*-dimethylformamide) ( $C222_1$ );  $[\text{ClSeNWCl}_5]^-$  ( $P2_1$ );  $[\text{I}(\text{N}_3)_2]^-$  ( $I_2$ );  $[\text{H}_3\text{GeNi}(\text{CO})_3]^-$  ( $C2$ );  $[\text{RuO}_2\text{Cl}_2(\text{O}_2\text{CMe})]^-$  ( $Cc$ );  $[\text{OsO}_4\text{Cl}]^- + \text{CH}_2\text{Cl}_2$  ( $P2/c$ );  $[\text{Cu}(\text{qdt})_2]^-$  (qdt = quinoxaline-2,3-dithiolate) +  $\text{H}_2\text{O}$  ( $P2/n$ );  $[\{\text{Me}_2\text{C}_6\text{H}_6(\text{OH})_2\}\text{PtCl}_3]^-$  ( $P2_1/c$ );  $[(\text{Me}_3\text{Si})_2\text{NMoNCl}_3]^-$  ( $P2_1/n$ );  $[\text{Ti}_2(\text{S}_4)_2]^{2-} + 2(\text{dmf})$  ( $P2_1/c$ );  $[\text{Se}_4\text{Br}_{12}]^{2-} + 2\text{CH}_2\text{Cl}_2$  ( $P2_1/c$ );  $[\text{B}_6\text{H}_5(\text{CH}_2\text{CH}_2\text{CH}_2)]^-$  (1,2-trimethylene-pentahydro-*closo*-hexaborate) ( $P\bar{1}$ );  $[(\eta^5\text{-C}_5\text{H}_5)\text{Mo}(\text{mnt})_2]^-$  (mnt = maleonitrile dithiolate) ( $P\bar{1}$ ). Note the considerable diversity of anions and crystal contents. This set of compounds reveals a new property of the LITQPE, namely slight variation from the linearity which is possible when the infinite quadruple phenyl embrace is propagated by a  $2_1$  screw axis rather than translation. There are four instances of this, with the  $\text{P} \cdots \text{P} \cdots \text{P}$  angle dropping to  $160^\circ$ .

#### Characteristics of ZZISPE chains

The zigzag sequence of  $\text{Ph}_4\text{P}^+$  cations, each interacting with its neighbour through an SPE comprising six concerted phenyl-phenyl interactions in edge-to-face conformation, is a common motif. As shown in Fig. 3, two phenyl rings on each  $\text{Ph}_4\text{P}^+$  are common to two contiguous SPEs, while the other two phenyl rings of  $\text{Ph}_4\text{P}^+$  each participate in only one SPE. In this paper we restrict attention to infinite chains of SPEs in crystals where

there are no additional phenyl embraces between the chains (that is  $\text{P} \cdots \text{P} > 9 \text{ \AA}$ ): because it is possible for one  $\text{Ph}_4\text{P}^+$  to participate in multiple phenyl embraces with more than two other  $\text{Ph}_4\text{P}^+$  cations, elaborate networks with multiple phenyl embraces between ZZISPE chains can occur, but these will be described separately.<sup>6</sup>

The zigzag geometry of the ZZISPE is a consequence of the tetrahedral geometry at P. Variation of the geometrical details in an SPE is possible,<sup>1,2</sup> and so there can be variation along a ZZISPE: the crystallographic repeat along the infinite chain in crystals can be one SPE, is commonly  $(\text{SPE})_2$ , and there is one crystal structure type with  $(\text{SPE})_{12}$  as the lattice repeat along the ZZISPE. Where the repeat is  $(\text{SPE})_2$  there is a unit cell dimension of ca. 11 Å. Instances of isolated ZZISPE chains are detailed in Table 4. The significant variables are (i) the  $\text{P} \cdots \text{P}$  distance in each SPE, (ii) the  $\text{P} \cdots \text{P} \cdots \text{P}$  angle between successive SPEs, (iii) the possible occurrence of symmetry elements along the chain, (iv) the repeat unit in the chain, and (v) the crystal packing arrangement of the ZZISPE chains. In all cases except one (DENZIF) the ZZISPE chains and stacks of anions are parallel to each other in the crystal lattice. There are two common packings of contiguous ZZISPE chains around the anion stacks, herringbone and parallel, as illustrated in Fig. 8. They are possible because the ZZISPE (unlike the LITQPE) possesses a plane defined by the P atoms, and rotations of the ZZISPEs around their axes change the mutual orientations of these planes: these variations are apparent in projection views along the ZZISPE chains, as in Fig. 8.

There are several important observations to be made on the occurrence and characteristics of the isolated ZZISPE chains. First, there is variety of anions in the instances presented in Table 4, ranging from the monatomic  $\text{Br}^-$  in its dihydrate (VAXFAB), to the large metal carbonyl cluster  $[(\mu_6\text{-C})\text{Os}_{10}(\text{CO})_{24}\text{HgCF}_3]^-$  (SEKVIN10), to hydrogen-bonded fluoroalcoholate  $[(\text{CF}_3)_2\text{C}(\text{OH})\text{O} \cdots (\text{HO})_2\text{C}(\text{CF}_3)_2]^-$  (DENZIF), to metal chelate complexes of various types. This variety of compounds will have a corresponding variety of intermolecular attractions which together with the ZZISPE

**Table 4** Characteristics of isolated ZZISPE chains in crystals. Distances are in Å and angles in °. P...P distances in bold have a centre of inversion at the midpoint. The repeat along the ZZISPE is (SPE)<sub>2</sub> unless noted otherwise. The compounds with the herringbone packing of ZZISPE [see Fig. 9(a)] are placed first in the table, then those with the parallel packing of ZZISPE [see Fig. 9(b)], followed by other types

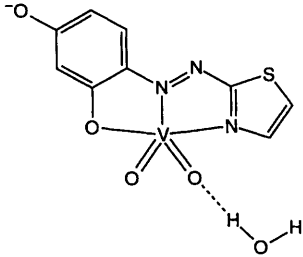
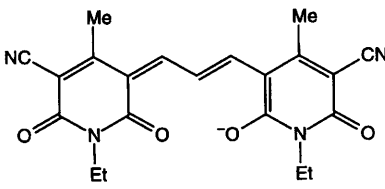
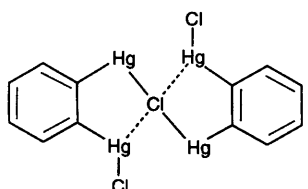
REFCODE	Anion, and other components	P...P distances	P...P...P angles	Space group	Packing type <sup>a</sup>
BALPEJ	[(WS <sub>4</sub> ) <sub>2</sub> Fe(dmf) <sub>2</sub> ] <sup>2-</sup>	<b>6.15, 6.95</b>	100.7	<i>P</i> 2 <sub>1</sub> / <i>n</i>	/
BEKYZ	[(Me <sub>2</sub> NNH <sub>2</sub> MoS <sub>4</sub> ) <sub>2</sub> Mo] <sup>2-</sup>	<b>6.08, 6.89</b>	99.9	<i>P</i> 2 <sub>1</sub> / <i>n</i>	/
DIBWOA	∞{[Hg <sub>2</sub> Te <sub>5</sub> ] <sup>2-</sup> }	6.30, 6.39	110.1	<i>P</i> 2 <sub>1</sub>	Infinite anion
VIPSOC	[Ni(Se <sub>4</sub> ) <sub>2</sub> ] <sup>2-</sup>	6.22, 6.67	116.0	<i>P</i> 2 <sub>1</sub>	/
JEXWEO	[Pd(Se <sub>4</sub> ) <sub>2</sub> ] <sup>2-</sup>	6.24, 6.68	116.8	<i>P</i> 2 <sub>1</sub>	Isomorphous with VIPSOC
HAXOF	[Pt(Se <sub>4</sub> ) <sub>2</sub> ] <sup>2-</sup>	6.14, 6.67	117.8	<i>P</i> 2 <sub>1</sub>	Isomorphous with VIPSOC
VIPSIW01	[Hg(Se <sub>4</sub> ) <sub>2</sub> ] <sup>2-</sup>	<b>6.42, 6.49<sup>b</sup></b>	108.3	<i>P</i> 2 <sub>1</sub> / <i>c</i>	/
JESMUP	[Cu <sub>2</sub> Se <sub>14</sub> ] <sup>4-</sup>	6.37, 6.51, 6.50, 6.52	109.2, 112.8, 113.8	<i>P</i> 2 <sub>1</sub>	/
JUWJIU	[Cu <sub>2</sub> Te <sub>12</sub> ] <sup>4-</sup>	<b>6.33</b> , 6.06, 6.52, 6.56, 6.39, 6.45, <b>6.44<sup>c</sup></b>	112.3, 112.2, 109.3, 108.0, 107.2, 113.0	<i>P</i> 2 <sub>1</sub> / <i>n</i>	Doubled
JUWJOA	[Ag <sub>2</sub> Te <sub>12</sub> ] <sup>4-</sup>	<b>6.36</b> , 6.05, 6.67, 6.63, 6.48, 6.46, <b>6.62<sup>c</sup></b>	114.0, 112.9, 109.6, 108.1, 106.9, 114.1	<i>P</i> 2 <sub>1</sub> / <i>n</i>	Isomorphous with JUWJIU
VAXFAB	Br <sup>-</sup> (H <sub>2</sub> O) <sub>2</sub>	<b>6.33<sup>d</sup></b>	117.4	<i>Pnma</i>	/
VIJVIT	[Ni(SCH <sub>2</sub> CH <sub>2</sub> S) <sub>2</sub> ] <sup>2-</sup> (H <sub>2</sub> O) <sub>4</sub>	<b>6.43, 6.89</b>	105.3	<i>P</i> 2 <sub>1</sub> / <i>c</i>	/
VOXWIO	[(μ-Cl) <sub>4</sub> (μ-S) <sub>2</sub> Sb <sub>4</sub> Cl <sub>6</sub> ] <sup>2-</sup>	<b>6.25, 6.74</b>	101.0	<i>P</i> 2 <sub>1</sub> / <i>c</i>	/
CEKSUG		<b>6.38, 6.51</b>	123.7	<i>P</i> $\bar{1}$	/
CEYSAA	[Fe(C <sub>2</sub> H <sub>3</sub> N <sub>3</sub> O <sub>2</sub> - <i>N, O</i> ) <sub>3</sub> ] <sup>-</sup>	6.79 <sup>e</sup>	145.6	<i>P</i> 2 <sub>1</sub>	/
DIBZET	[Au <sub>4</sub> Te <sub>4</sub> ] <sup>4-</sup> (dmf) <sub>2</sub> (MeOH) <sub>2</sub> cations are [Ph <sub>4</sub> P <sup>+</sup> ] <sub>2</sub> [K <sup>+</sup> ] <sub>2</sub>	<b>5.93, 6.60</b>	101.7	<i>P</i> $\bar{1}$	/
DICCIB	[(SCH <sub>2</sub> CH <sub>2</sub> S) <sub>2</sub> VS] <sup>2-</sup> (Et <sub>2</sub> O) <sub>x</sub> cations are Ph <sub>4</sub> P <sup>+</sup> and Na <sup>+</sup>	<b>6.23, 6.54</b>	101.9	<i>P</i> $\bar{1}$	/
FUMDUM	[(N <sub>3</sub> ) <sub>2</sub> Cu(N <sub>3</sub> ) <sub>2</sub> Cu(N <sub>3</sub> ) <sub>2</sub> ] <sup>2-</sup>	<b>6.10, 6.42</b>	129.3	<i>P</i> $\bar{1}$	/
GAHZEU	[As <sub>3</sub> S <sub>3</sub> Cl <sub>4</sub> ] <sup>-</sup>	<b>6.46, 6.73</b>	128.5	<i>P</i> $\bar{1}$	/
GAHZIY	[As <sub>3</sub> S <sub>3</sub> Br <sub>4</sub> ] <sup>-</sup>	<b>6.48, 6.62</b>	117.4	<i>P</i> $\bar{1}$	Isomorphous with GAHZEU
GOJJAQ	[(18-crown-6)(VCl <sub>4</sub> ) <sub>2</sub> ] <sup>2-</sup> (CH <sub>2</sub> Cl <sub>2</sub> ) <sub>4</sub>	<b>6.44, 6.71</b>	121.9	<i>P</i> $\bar{1}$	/
KUXPOI	[(Me <sub>3</sub> SiN) <sub>2</sub> (TiCl <sub>3</sub> ) <sub>2</sub> ] <sup>2-</sup> MeCN	<b>6.62, 6.64</b>	101.9	<i>P</i> $\bar{1}$	/



Table 4 (continued)

REFCODE	Anion, and other components	P...P distances	P...P...P angles	Space group	Packing type <sup>a</sup>
SEKVIN10	$[(\mu_6\text{-C})\text{Os}_{10}(\text{CO})_{24}\text{HgCF}_3]^-$	<b>6.32, 6.32</b>	139.5	$P\bar{1}$	/ / Large separation of ZZISPE, at 16.0, 17.5; see Fig. 9
WEKKUS	$[(\mu_3\text{-Br})_8\text{Mo}_6\text{F}_6]^{2-} (\text{H}_2\text{O})_2$	<b>6.27, 6.58</b>	99.7	$P\bar{1}$	/ /
SOTFAI	$[\text{C}_{21}\text{H}_{19}\text{N}_4\text{O}_4]^-$	<b>6.97<sup>f</sup></b>	135.1 <sup>g</sup>	$P2_1/c$	/ /
					/ /
JAXYAI10	$[\text{Ni}_3(\text{MeCHSCH}_2\text{S})_4]^{2-} (\text{MeCN})_2$	6.54 <sup>e</sup>	98.6	$P2_1/c$	 0-0-0     0-0-0 
CUFCEL10	$[(\mu_4\text{-Cl})(\text{HgC}_6\text{H}_4\text{HgCl}_2)]^- \text{CH}_2\text{Cl}_2$	<b>6.15, 6.99, 6.44<sup>h</sup></b>	111.2, 124.0	$P\bar{1}$	Neither pattern
					
CUSPOV	$[(\text{SCH}_2\text{CH}_2\text{S})_2\text{VS}]^{2-} \text{MeOH}$	<b>6.17, 6.82</b>	108.5	$P\bar{1}$	<i>i</i>
DENZIF	$[(\text{CF}_3)_2\text{C}(\text{OH})\text{O} \cdots (\text{HO})_2\text{C}(\text{CF}_3)_2]^-$	<b>6.90<sup>f</sup></b>	131.3	$I4_1/a$	Two orthogonal, identical ZZISPE in the cell: H bonding present
DOFWEA	$[\text{Mn}_3(\text{SCH}_2\text{CH}_2\text{S})_5]^{2-}$	<b>5.88, 6.98</b>	100.1	$P\bar{1}$	<i>g</i>
JANZED	$[(\text{MeO}_2\text{C})_2\text{C}_2\text{Te}_2\text{MoO}]^{2-} \text{thf}$	<b>6.44, 6.62, 6.43, 6.51</b>	122.9, 124.7	$P\bar{1}$	 0 0       0 0
		two similar chains			
PERBET	$[(\mu\text{-CO})(\mu\text{-C}_6\text{Cl}_4\text{S}_2)\text{Cr}_2(\text{CO})_6]^{2-} \text{MeCN}$	<b>6.58, 6.66, 6.22<sup>h</sup></b>	143.0, 116.6	$P2_1/n$	Neither of the usual patterns; similar to CUFCEL10
SAKTON	$[(\text{SCH}_2\text{CH}_2\text{S})_3\text{Cu}_4]^{2-} \text{MeOH}$	<b>6.19, 6.22</b>	122.3	$P\bar{1}$	Isolated ZZISPE plus other multiple phenyl embraces in cell
YASWUK	$[(\text{SCH}_2\text{CH}_2\text{S})_3\text{Cu}_4]^{2-}$	<b>5.98, 6.19</b>	126.9	$P\bar{1}$	Like SAKTON
YASXAR	$[(\text{SCH}_2\text{CH}_2\text{S})_3\text{Cu}_4]^{2-} \text{MeOH}$	<b>6.42, 6.74</b>	127.8	$P\bar{1}$	Like SAKTON
VECHAM10	$[\text{W}(\text{CN})_5(\text{OME})]^{2-}$	<b>6.04, 6.38</b>	119.1	$P\bar{1}$	<i>i</i>

(18-crown-6) = 1,4,7,10,13,16-hexaoxacyclooctadecane. <sup>a</sup> The symbols represent the orientations of the P planes of each ZZISPE: see Fig. 8.

\ / \ = VIPSOC herringbone, pattern of Fig. 8(a); / / = GAHZEU parallel, pattern of Fig. 8(b). <sup>b</sup> There is a second, poorer, ZZISPE with

P...P distances of 6.32, 7.14 Å, and a P...P...P angle of 101.7°. <sup>c</sup> The ZZISPE repeats after 12 SPEs. <sup>d</sup> A mirror plane passes through  $\text{Ph}_4\text{P}^+$ , and a  $2_1$  axis propagates the ZZISPE. <sup>e</sup> The ZZISPE is generated by the  $2_1$  operation on one SPE. <sup>f</sup> The ZZISPE has a two-fold axis perpendicular to the chain, through  $\text{Ph}_4\text{P}^+$ . <sup>g</sup> A borderline offset sextuple phenyl embrace, OSPE. <sup>h</sup> The repeat unit along the ZZISPE is four SPEs, comprised of two different centrosymmetric SPEs separated by one type of non-centrosymmetric SPE: there are two unique P...P...P angles. <sup>i</sup> In addition to the ZZISPE there are other more complex layers of SPE in this cell.

provide the cohesive energy for the lattice, but the repeated occurrence of the ZZISPE in this variety of compounds attests to its stability. Many of the crystal lattices in Table 4 contain solvent, and two lattices contain in addition alkali-metal cations, but these additions do not interfere with the ZZISPEs.

A more dramatic illustration of the stability of the isolated ZZISPE occurs in  $[\text{Ph}_4\text{P}][(\mu_6\text{-C})\text{Os}_{10}(\text{CO})_{24}\text{HgCF}_3]$

(SEKVIN 10) for which the lattice packing viewed along the ZZISPE columns is presented in Fig. 9.\* Here the ZZISPE chains are completely separated by intervening sections of the large cluster anions.

\* The ZZISPE in SEKVIN10 is distorted, such that alternate SPEs are more like offset-sextuple-phenyl embraces (OSPE).<sup>2</sup>

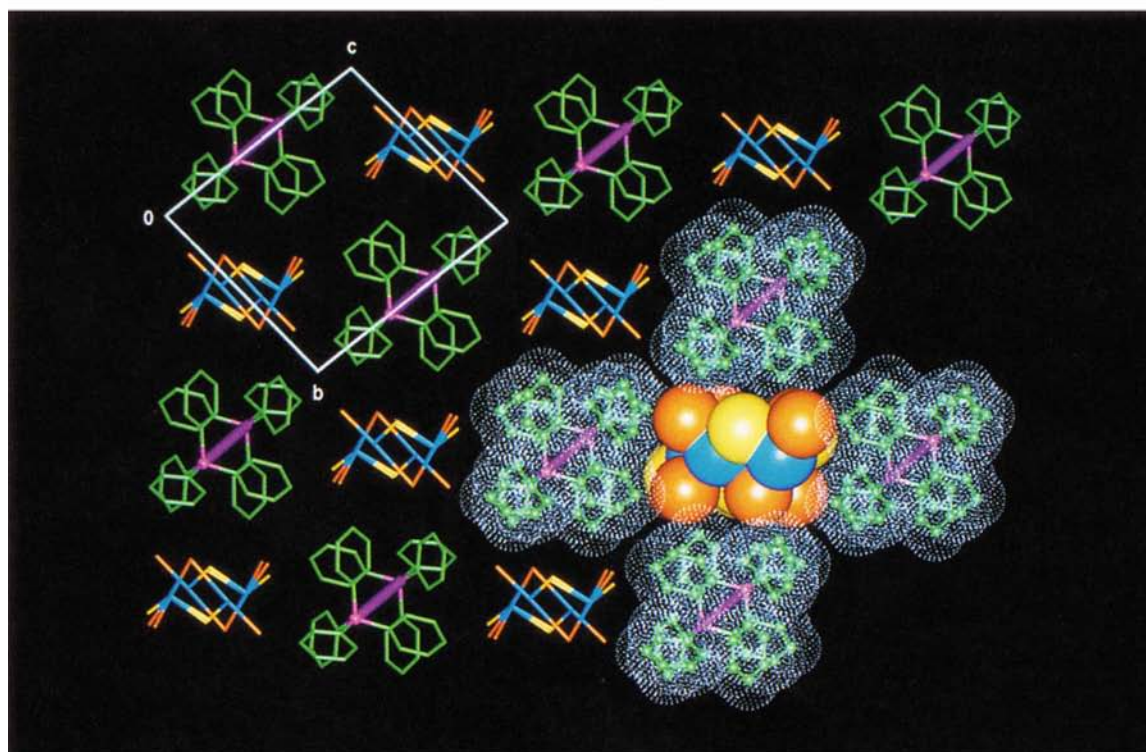
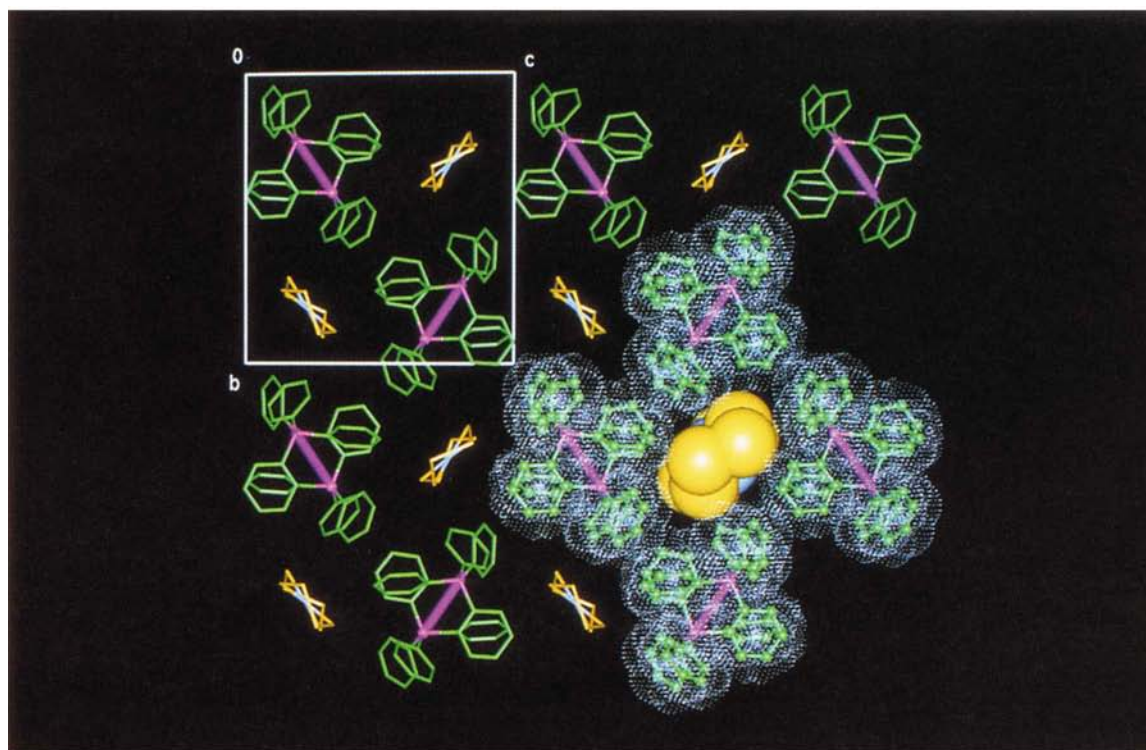


**Fig. 8** Two common crystal packing arrangements for isolated ZZISPE chains. (a) Herringbone array of ZZISPE planes, as occurs in  $[\text{Ph}_4\text{P}]_2[\text{Ni}(\text{Se}_4)_2]$  (VIPSOC): the pseudo-planar anion is oriented edge-on in the cavity between four ZZISPE chains, and only the Se atoms are visible. (b) Parallel array of ZZISPE planes, as occurs in  $[\text{Ph}_4\text{P}][\text{As}_3\text{S}_3\text{Cl}_4]$  (GAHZEU): As blue, S yellow, Cl orange

The one instance of non-parallel isolated ZZISPE chains occurs in DENZIF, which contains  $[(\text{CF}_3)_2\text{C}(\text{OH})\text{O}]^-$  hydrogen bonded with  $(\text{CF}_3)_2\text{C}(\text{OH})_2$  as a large anion with a largely fluorinated surface. As shown in Fig. 10, there are ZZISPE chains running in two orthogonal directions (the crystal system is tetragonal) around the anions.

For the more regular structures with parallel ZZISPEs, the

two crystal isomers arising from ZZISPE rotation, shown in Fig. 8, both occur generally and their listings are segregated in Table 4. The herringbone array [Fig. 8(a)] is adopted more by the metal polychalcogenide compounds, usually in a monoclinic space group with  $2_1$  axes, while the ZZISPE array with parallel  $P_\infty$  planes [Fig. 8(b)] is adopted by metal chelate complexes and more diverse anions, usually in space group  $P\bar{1}$ .

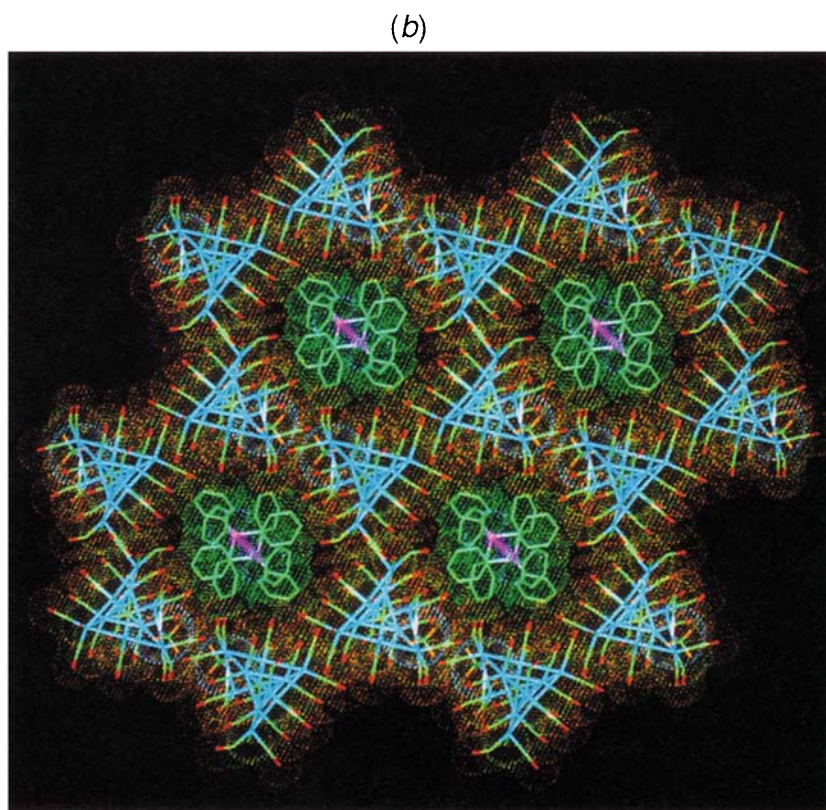
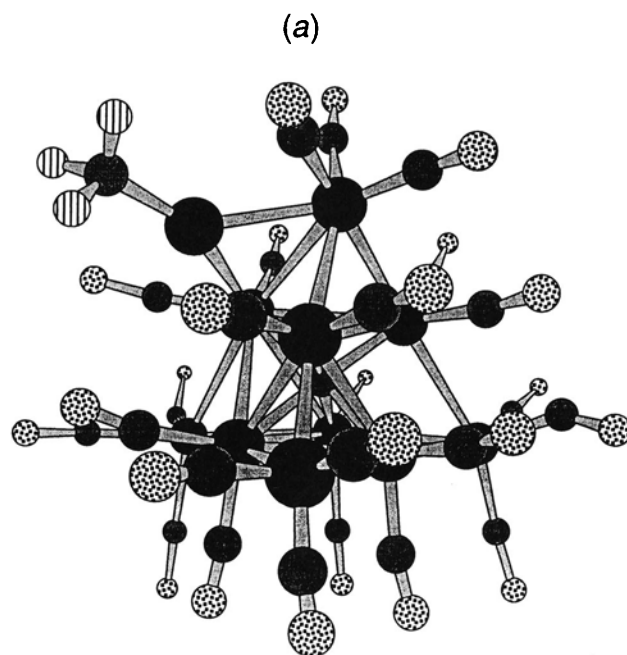


**Fig. 9** (a) Molecular structure of the anion  $[(\mu_6\text{-C})\text{Os}_{10}(\text{CO})_{24}\text{HgCF}_3]^-$ : F vertical stripes, O speckled. (b) Projection of the crystal structure of  $[\text{Ph}_4\text{P}][(\mu_6\text{-C})\text{Os}_{10}(\text{CO})_{24}\text{HgCF}_3]$  (SEKVIN10) along the ZZISPE chains. The blue atoms are Os, Hg is lavender, and the carbonyl oxygen atoms on the surface of the cluster anion are red

Attention is directed also to the remarkable crystal lattices adopted by the copper and silver polyselenides and polytellurides, JESMUP, JUWJIU and JUWJOA. These contain tetraanions, relatively small with  $\text{E}_4$  and  $\text{E}_5$  ligands ( $\text{E} = \text{Se}$  or  $\text{Te}$ ) around two metal atoms, and crystallised with

four  $\text{Ph}_4\text{P}^+$  cations: the proportion of the cell volume occupied by the cations is relatively large, and yet the ZZISPEs are isolated. In JESMUP there are four distinct SPEs along the ZZISPE, while isomorphous JUWJIU and JUWJOA have twelve SPEs along the ZZISPE before there is translational

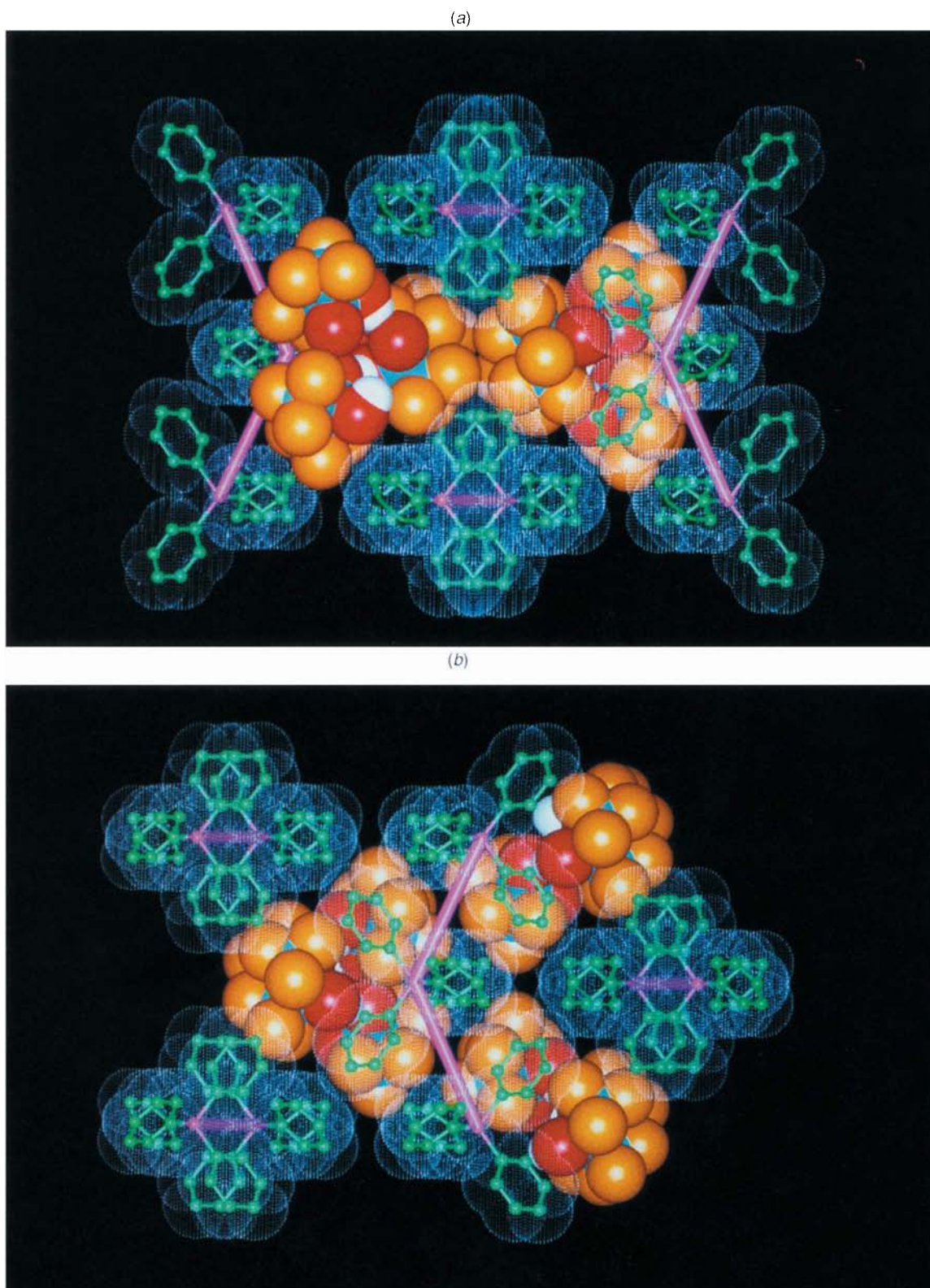


**Fig. 10** Two orthogonal views of the crystal structure of  $[(\text{CF}_3)_2\text{C}(\text{OH})\text{O}\cdots(\text{HO})_2\text{C}(\text{CF}_3)_2]^-$  showing the isolated ZZISPE chains running in orthogonal directions; F orange, C (in the anion) blue, O red; the purple rods connect the P atoms along the ZZISPE chains. The second view (b) is rotated  $90^\circ$  about the horizontal axis relative to (a)

repetition. This latter structure type occurs in a  $P2_1/n$  cell,  $17 \times 17 \times 51 \text{ \AA}$ ,  $94^\circ$ , with two different centres of inversion along the ZZISPE (see Table 4).

#### Through-space interaction energies

The foregoing analyses of crystal supramolecularity based on infinite multiple phenyl embraces have been conveniently based

on geometry, but it is the interaction energies which determine structure. Therefore calculations of relevant through-space energies have been made for representative LITQPE and ZZISPE structures, namely  $\text{Ph}_4\text{P}^+\text{Br}^-$  (DEMYEZ) in class  $\bar{I}4$ ,  $\text{Ph}_4\text{P}^+[\text{SnbCl}_4]^-$  (CETBAE) in class  $P4/n$  {CETBAE packing},  $\text{Ph}_4\text{P}^+[\text{NbCl}_6]^-$  (PCLNBA) in class  $P4/n$  {GAYZUB packing},  $\text{Ph}_4\text{P}^+[\text{NbBr}_6]^-$  (PSBRNB) in class  $C2/c$ , and  $\text{Ph}_4\text{P}^+[\text{As}_3\text{S}_3\text{Cl}_4]^-$  (GAHZEU), a ZZISPE. The

**Table 5** Through-space (non-bonded) interaction energies (kcal mol<sup>-1</sup>) between nearest ions in representative crystals containing LITQPE columns or ZZISPE chains. Ph1, Ph2, Ph3, Ph4 refer to the four phenyl rings on each cation; primes signify rings on the reference cation. Total energies between cations are expressed per [Ph<sub>4</sub>P<sup>+</sup>]<sub>2</sub> pair

Ph<sub>4</sub>P<sup>+</sup>Br<sup>-</sup> DEMYEZ

Ph <sub>4</sub> P <sup>+</sup>	To nearest Ph <sub>4</sub> P <sup>+</sup> along LITQPE				
	Ph1	Ph2	Ph3	Ph4	P
Ph1'	-0.1	-0.6	-3.4	-3.4	+0.2
Ph2'	-0.6	-0.1	-3.4	-3.4	+0.2
Ph3'	0	0	-0.1	-0.6	+0.1
Ph4'	0	0	-0.6	-0.1	+0.1
P'	+0.1	+0.1	+0.2	+0.2	+1.1

\* Single ef interaction per Ph<sub>4</sub>P<sup>+</sup> between contiguous LITQPE columns.

Total (Ph)<sub>4</sub> to (Ph)<sub>4</sub> along LITQPE = -16.4  
Total [Ph<sub>4</sub>P] to [Ph<sub>4</sub>P] along LITQPE = -14.1

Anion to nearest Ph<sub>4</sub>P<sup>+</sup>

	Ph1	Ph2	Ph3	Ph4	P
Anion	-0.6	-3.6	-3.5	-0.5	-3.5

Ph<sub>4</sub>P<sup>+</sup>[SNbCl<sub>4</sub>]<sup>-</sup> CETBAE

Ph <sub>4</sub> P <sup>+</sup>	To nearest Ph <sub>4</sub> P <sup>+</sup> along LITQPE				
	Ph1	Ph2	Ph3	Ph4	P
Ph1'	-0.4	-0.1	-3.3	-3.3	+0.4
Ph2'	-0.1	-0.4	-3.3	-3.3	+0.4
Ph3'	0	0	-0.4	-0.1	+0.1
Ph4'	0	0	-0.1	-0.4	+0.1
P'	+0.1	+0.1	+0.4	+0.4	+0.9

\* Weak vertex-to-face interaction between contiguous LITQPE columns.

Total (Ph)<sub>4</sub> to (Ph)<sub>4</sub> along LITQPE = -15.2  
Total [Ph<sub>4</sub>P] to [Ph<sub>4</sub>P] along LITQPE = -12.3

Anion to nearest Ph<sub>4</sub>P<sup>+</sup>

	Ph1	Ph2	Ph3	Ph4	P
Anion	-2.4	-4.5	-2.4	-0.5	-3.7

Ph<sub>4</sub>P<sup>+</sup>[NbCl<sub>6</sub>]<sup>-</sup> PCLNBA

Ph <sub>4</sub> P <sup>+</sup>	To nearest Ph <sub>4</sub> P <sup>+</sup> along LITQPE				
	Ph1	Ph2	Ph3	Ph4	P
Ph1'	-0.3	-3.2	-0.1	-3.2	+0.4
Ph2'	0	-0.3	0	-0.1	+0.1
Ph3'	-0.1	-3.2	-0.3	-3.2	+0.4
Ph4'	0	-0.1	0	-0.3	+0.1
P'	+0.1	+0.4	+0.1	+0.4	+0.9

Total (Ph)<sub>4</sub> to (Ph)<sub>4</sub> along LITQPE = -14.4  
Total [Ph<sub>4</sub>P] to [Ph<sub>4</sub>P] along LITQPE = -11.5

Anion to nearest Ph<sub>4</sub>P<sup>+</sup>

	Ph1	Ph2	Ph3	Ph4	P
Anion	-3.6	-3.3	-2.1	-0.5	-3.8

Ph<sub>4</sub>P<sup>+</sup>[NbBr<sub>6</sub>]<sup>-</sup> (PSBRNB)

Ph <sub>4</sub> P <sup>+</sup>	To nearest Ph <sub>4</sub> P <sup>+</sup> along LITQPE				
	Ph1	Ph2	Ph3	Ph4	P
Ph1'	-0.8	0	-0.1	0	+0.1
Ph2'	-3.1	-0.7	-2.6	-0.1	+0.2
Ph3'	-0.1	0	-0.8	0	+0.1
Ph4'	-2.6	-0.1	-3.1	-0.7	+0.2
P'	+0.2	+0.1	+0.2	+0.1	+1.1

\* Offset face-to-face interaction between contiguous LITQPE columns.

Total (Ph)<sub>4</sub> to (Ph)<sub>4</sub> along LITQPE = -14.8  
Total [Ph<sub>4</sub>P] to [Ph<sub>4</sub>P] along LITQPE = -12.5

Anion to nearest Ph<sub>4</sub>P<sup>+</sup>

	Ph1	Ph2	Ph3	Ph4	P
Anion	-1.0	-2.1	-0.6	-4.1	-3.3

To nearest Ph<sub>4</sub>P<sup>+</sup> in different LITQPE

Ph1	Ph2	Ph3	Ph4	P
0	0	0	0	+0.1
0	0	0	0	+0.2
-1.2	-0.7	-0.1	-3.4*	+0.6
0	0	0	0	+0.1
+0.3	+0.3	+0.1	+0.2	+0.6

Total (Ph)<sub>4</sub> to (Ph)<sub>4</sub> in different LITQPE = -5.4  
Total [Ph<sub>4</sub>P] to [Ph<sub>4</sub>P] in different LITQPE = -2.9

Total

-11.7

To nearest Ph<sub>4</sub>P<sup>+</sup> in different LITQPE

Ph1	Ph2	Ph3	Ph4	P
-0.1	0	-1.7*	0	+0.2
-1.7*	-0.1	-0.6	0	+0.5
0	0	-0.1	0	+0.1
0	0	0	0	+0.1
+0.2	+0.1	+0.5	+0.1	+0.6

Total (Ph)<sub>4</sub> to (Ph)<sub>4</sub> in different LITQPE = -4.3  
Total [Ph<sub>4</sub>P] to [Ph<sub>4</sub>P] in different LITQPE = -1.9

Total

-13.5

To nearest Ph<sub>4</sub>P<sup>+</sup> in different LITQPE

Ph1	Ph2	Ph3	Ph4	P
-0.2	0	0	0	+0.1
-1.4	-0.2	0	-1.3	+0.6
-1.3	0	0	-0.1	+0.2
0	0	0	0	+0.1
+0.6	+0.1	+0.1	+0.2	+0.6

Total (Ph)<sub>4</sub> to (Ph)<sub>4</sub> in different LITQPE = -4.5  
Total [Ph<sub>4</sub>P] to [Ph<sub>4</sub>P] in different LITQPE = -1.9

Total

-13.3

To nearest Ph<sub>4</sub>P<sup>+</sup> in different LITQPE

Ph1	Ph2	Ph3	Ph4	P
0	0	0	-0.3	+0.1
0	0	0	-1.0	+0.2
-0.3	-0.1	-1.0	-4.9*	+0.6
0	0	0	-0.1	+0.1
+0.1	+0.1	+0.2	+0.6	+0.6

Total (Ph)<sub>4</sub> to (Ph)<sub>4</sub> in different LITQPE = -7.7  
Total [Ph<sub>4</sub>P] to [Ph<sub>4</sub>P] in different LITQPE = -5.1

Total

-11.1

Table 5 (continued)

Ph <sub>4</sub> P <sup>+</sup> [As <sub>3</sub> S <sub>3</sub> Cl <sub>4</sub> ] <sup>-</sup> GAHZEU										
Ph <sub>4</sub> P <sup>+</sup>	One SPE in ZZISPE repeat					Other SPE in ZZISPE repeat				
	Ph1	Ph2	Ph3	Ph4	P	Ph1	Ph2	Ph3	Ph4	P
Ph1'	-1.5	-0.4	-0.1	-3.6	+0.5	-1.8	-0.4	-3.4	-0.1	+0.5
Ph2'	-0.3	-1.5	-0.1	-3.4	+0.1	-0.3	-1.8	-2.9	-0.1	+0.2
Ph3'	-0.1	-0.1	0	-0.1	+0.1	-2.9	-3.4	-0.8	-0.1	+0.2
Ph4'	-3.4	-3.6	-0.1	-0.9	+0.1	-0.1	-0.1	-0.1	0	+0.1
P'	+0.1	+0.5	+0.1	+0.1	+1.2	+0.2	+0.5	+0.2	+0.1	+1.2
Ph <sub>4</sub> P <sup>+</sup>	To nearest Ph <sub>4</sub> P <sup>+</sup> in different ZZISPE									
	Ph1	Ph2	Ph3	Ph4	P					
Ph1'	0	0	-0.2	0	+0.1					
Ph2'	0	0	-1.8	-0.2	+0.5					
Ph3'	0	0	0	0	+0.1					
Ph4'	0	0	0	0	+0.1					
P'	+0.1	+0.1	+0.5	+0.1	+0.5					
Total (Ph) <sub>4</sub> to (Ph) <sub>4</sub> in SPE interactions along ZZISPE = -19.2, -18.3						Total (Ph) <sub>4</sub> to (Ph) <sub>4</sub> in different ZZISPE = -2.2				
Total [Ph <sub>4</sub> P] to [Ph <sub>4</sub> P] in SPE interactions along ZZISPE = -16.4, -15.1						Total [Ph <sub>4</sub> P] to [Ph <sub>4</sub> P] in different ZZISPE = -0.1				
Anion to nearest Ph <sub>4</sub> P <sup>+</sup>										
	Ph1	Ph2	Ph3	Ph4	P	Total				
Anion	-6.6	-0.6	-4.7	-5.1	-5.3	-22.3				

intermolecular energies are evaluated (as sums of atom-atom through-space energies: see Methodology section) between phenyl rings, P atoms, and total ions as the chemical entities. The results are provided in detail in Table 5, in order to emphasise the components and the totals of the interaction energies, and the results are segregated according to (i) cation to cation along the LITQPE or ZZISPE, (ii) cation to the nearest cation in a different LITQPE or ZZISPE, and (iii) anion to nearest cation. For each Ph<sub>4</sub>P<sup>+</sup> to Ph<sub>4</sub>P<sup>+</sup> interaction the (Ph)<sub>4</sub> to (Ph)<sub>4</sub> energies are attractive, and are diminished slightly (2–3 kcal mol<sup>-1</sup>) by the inclusion of P contributions. Note that Ph<sub>4</sub>P<sup>+</sup> cations are mutually attractive, not repulsive.

In the four LITQPE examples the [Ph<sub>4</sub>P]-to-[Ph<sub>4</sub>P] interaction within the LITQPE ranges from -11.5 to -14.1 kcal mol<sup>-1</sup> per [Ph<sub>4</sub>P<sup>+</sup>]<sub>2</sub> pair. The closest [Ph<sub>4</sub>P]-to-[Ph<sub>4</sub>P] interaction between LITQPEs has values -1.9, -1.9, -2.9 and -5.1 kcal mol<sup>-1</sup> per [Ph<sub>4</sub>P<sup>+</sup>]<sub>2</sub> pair, the higher value in the last (PSBRNB) being due to a single offset face-to-face interaction. The interaction energies between cation and anion range from -11.1 to -13.5 kcal mol<sup>-1</sup> per cation-anion pair.

An SPE is more attractive than a QPE.<sup>2</sup> In Ph<sub>4</sub>P<sup>+</sup>-[As<sub>3</sub>S<sub>3</sub>Cl<sub>4</sub>]<sup>-</sup> the intraZZISPE energies are -16.4 and -15.1 kcal mol<sup>-1</sup> per [Ph<sub>4</sub>P<sup>+</sup>]<sub>2</sub> pair, in stark contrast to the most favourable interZZISPE energy of -0.1 kcal mol<sup>-1</sup> per [Ph<sub>4</sub>P<sup>+</sup>]<sub>2</sub> pair, while the closest anion-cation pair has an energy of -22.3 kcal mol<sup>-1</sup>.

The general conclusion is that the through-space attractions between Ph<sub>4</sub>P<sup>+</sup> cations along the LITQPE and ZZISPE motifs are major contributors to the crystal lattice energy, together with the cation-anion attractions, whereas the intermotif attractions between Ph<sub>4</sub>P<sup>+</sup> cations make minor contributions. While a complete calculation of the lattice-packing energy must include all through-space interactions, to long distances, our evaluation of local attractions provides a semi-quantitative view of the dominant energetics in these crystals, and demonstrates the significance of the supramolecular motifs involving multiple phenyl embraces.

## Discussion

We summarise our main findings.

(1) Infinite sequences of multiple phenyl embraces involving Ph<sub>4</sub>P<sup>+</sup> cations are prevalent in crystals, and in 88 crystals these

infinite sequences are well separated from each other. Of these, 52 crystals contained repeated quadruple phenyl embraces (QPE), and 36 crystals repeated sextuple phenyl embraces (SPE).<sup>\*</sup> (2) The linear infinite translational quadruple phenyl embraces, LITQPE, occur as columns which with few exceptions are linear due to crystallographic translation, while the zigzag infinite sextuple phenyl embraces, ZZISPE, are zigzag chains in which the P atoms are coplanar. (3) The predominant crystal packing arrangement has stacks of anions (sometimes alternating with solvent molecules) between and parallel to the columns of LITQPE or chains of ZZISPE. In two instances the anion is one-dimensionally non-molecular, along the stack, and commensurate with the LITQPE or ZZISPE. (4) 23 Crystals containing the LITQPE have a tetragonal lattice, and these can be classified according to the packing of cation columns and anion stacks in space groups *P4/n* (with moderately sized anions with point symmetry *C*<sub>4</sub>, and longer P...P distances in the QPE) and *I*<sub>4</sub> (with small anions, usually with point symmetry *S*<sub>4</sub>, and shorter P...P distances in the QPE). In the LITQPE packing classes there are subtleties arising from rotation around the columns, and in the *P4/n* class this crystal isomerism is correlated with the shape (mushroom or spherical) of the anion. (5) A class of LITQPE occurs in space group *C2/c*, where there are lesser symmetry requirements for the anion. (6) There are four structures in which the LITQPE is propagated by a 2<sub>1</sub> screw element rather than translation, allowing slight non-linearity. (7) A characteristic of crystals containing LITQPE is a cell dimension in the range 6.7 to 7.8 Å, which is the P...P distance of the QPE. (8) The crystallographic repeat for a ZZISPE is usually (SPE)<sub>2</sub>, but can be (SPE)<sub>1</sub> up to (SPE)<sub>12</sub>. The (SPE)<sub>2</sub> repeat usually results in a cell dimension of ca. 11 Å. (9) Zigzag infinite sextuple phenyl embraces occur with a variety of anions, small and large, and demonstrate crystal isomerism due to rotation about the ZZISPE axis. (10) Crystallographic disorder of cations is not observed, consistent with the integrity of the LITQPE and ZZISPE motifs, but orientational disorder (and in one instance translational disorder) of anions can occur. (11) The

\* The large number of crystals containing interacting infinite sequences, that is networks of multiple phenyl embraces, will be described subsequently.<sup>6</sup>

separations of LITQPE columns and ZZISPE chains are variable: the columns and chains can be well separated by anion space. (12) *Attractions between cations* are major contributors to crystal cohesion. Through-space interaction energies for representative crystals containing LITQPE and ZZISPE motifs indicate that the *intramotif* multiple phenyl embraces between  $\text{Ph}_4\text{P}^+$  cations are major attractive energies, and much larger than the *intermotif* attractive energies. The energy components are *ca.*  $-13 \text{ kcal mol}^{-1}$  per  $[\text{Ph}_4\text{P}^+]_2$  pair for a LITQPE and *ca.*  $-16 \text{ kcal mol}^{-1}$  per  $[\text{Ph}_4\text{P}^+]_2$  pair for a ZZISPE: these attractive energies are of similar magnitude to those between adjacent cation-anion pairs in the crystals calculated. The *intermotif* energies are much less, *ca.*  $-1$  to  $-3 \text{ kcal mol}^{-1}$  per cation pair.

## Conclusion

We conclude that the variety of packing arrangements for the LITQPE columns and ZZISPE chains, together with the through-space energies, demonstrate that these concerted supramolecular motifs are inherently stable. We believe that they are supramolecular crystal tectons<sup>18,19</sup> (or synthons<sup>20</sup>) for compounds containing  $\text{Ph}_4\text{P}^+$ . In the crystals which contain LITQPEs and ZZISPEs, hydrogen bonding is usually absent, and is not a significant feature of this crystal supramolecularity. The crystals we have tabulated are akin to hydrophobic assemblies, but they are distinctive in necessarily containing ions: their classification in supramolecular chemistry is with the hydrophobic salts.\*

The attractive energies of the multiple phenyl embraces involving  $\text{Ph}_4\text{P}^+$  are greater than the energies of most hydrogen bonds.<sup>21</sup>

We make two points about the significance of our findings. First, can we predict the crystal structures of salts containing  $\text{Ph}_4\text{P}^+$ , and undertake crystal engineering? While the classifications and patterns evident in this paper allow some prediction, mainly by analogy with tabulated compounds, full predictive power depends on an understanding of all of the types of crystal structures containing  $\text{Ph}_4\text{P}^+$ . There are other more elaborate networks of multiple phenyl embraces involving  $\text{Ph}_4\text{P}^+$  which will be described later.<sup>6</sup> The next stage of the analysis also involves considerations of anion properties (size per negative charge, and shape).

Secondly, we note that in our approach to supramolecular motifs in molecular crystals of diverse compounds we are, in effect, revealing crystal packing relationships, and uncovering crystal lattices which despite chemical differences are virtually isomorphous. This is done not by primary analysis of lattice

\* The multiple phenyl embraces of  $\text{Ph}_4\text{P}^+$  also occur for  $\text{Ph}_3\text{E}$  ligands and  $\text{Ph}_2\text{E}$  moieties,<sup>1</sup> and thus contribute to attractive motifs in other divisions of supramolecular chemistry.

dimensions or of space groups, but by investigation of the local supramolecular interactions. We believe that this approach has value because it mimics the crystallisation process.†

## Acknowledgements

This research is supported by grants from the Australian Research Council.

† *Note added at proof:* the symmetries and dimensions for the tetragonal lattices which contain columns of cations have been classified previously.<sup>22</sup>

## References

- 1 I. G. Dance and M. L. Scudder, *J. Chem. Soc., Chem. Comm.*, 1995, 1039.
- 2 I. G. Dance and M. L. Scudder, *Chem. Eur. J.*, 1996, **2**, 481.
- 3 N. A. Ahmed, A. I. Kitaigorodski and K. V. Mirskaya, *Acta Crystallogr., Sect. B*, 1971, **27**, 867.
- 4 W. B. Schweizer, in *Structure Correlation*, eds. H.-B. Burgi and J. D. Dunitz, VCH, Weinheim, 1994, ch. 9.
- 5 F. H. Allen, J. E. Davies, J. J. Galloy, O. Johnson, O. Kennard, C. F. Macrae, E. M. Mitchell, G. F. Mitchell and D. G. Watson, *J. Chem. Inf. Comput. Sci.*, 1991, **31**, 187.
- 6 I. G. Dance and M. L. Scudder, unpublished work.
- 7 G. R. Desiraju, *Crystal Engineering: The Design of Organic Solids*, Elsevier, Amsterdam, 1989.
- 8 *Structure Correlation*, eds. H. B. Burgi and J. D. Dunitz, VCH, Weinheim, 1994.
- 9 I. G. Dance, in *The Crystal as a Supramolecular Entity*, ed. G. Desiraju, Wiley, Chichester, 1996.
- 10 Catalysis, Molecular Simulations Inc., San Diego, CA, 1995.
- 11 Program Discover, Molecular Simulations Inc., San Diego, CA, 1995.
- 12 A. J. Pertsin and A. I. Kitaigorodski, *The Atom-Atom Potential Method. Applications to Organic Molecular Solids*, Springer, Berlin, 1987.
- 13 P. Comba and T. W. Hambley, *Molecular Modeling of Inorganic Compounds*, VCH, Weinheim, 1995.
- 14 N. L. Allinger, *Adv. Phys. Org. Chem.*, 1976, **13**, 1.
- 15 D. Gizachew and I. G. Dance, unpublished work.
- 16 Program DMol v. 2.36, Molecular Simulations Inc., San Diego, CA, 1995.
- 17 E. E. Schweizer, C. J. Baldacchini and A. L. Rheingold, *Acta Crystallogr., Sect. C*, 1989, **45**, 1236.
- 18 M. Simard, D. Su and J. D. Wuest, *J. Am. Chem. Soc.*, 1991, **113**, 4696.
- 19 A. Muller, H. Reuter and S. Dillinger, *Angew. Chem., Int. Ed. Engl.*, 1995, **34**, 2328.
- 20 G. R. Desiraju, *Angew. Chem., Int. Ed. Engl.*, 1995, **34**, 2311.
- 21 J. E. Huheey, *Inorganic Chemistry*, 3rd edn., Harper, 1983; C. B. Aakeroy and K. R. Seddon, *Chem. Soc. Rev.*, 1993, 397; H. Schneider, *Angew. Chem., Int. Ed. Engl.*, 1991, **30**, 1417; J. S. Lindsey, *New J. Chem.*, 1991, **15**, 153.
- 22 U. Muller, *Acta Crystallogr., Sect. B*, 1980, **36**, 1075.

Received 25th March 1996; Paper 6/02040B